

Molecular Physics

An International Journal at the Interface Between Chemistry and Physics

ISSN: 0026-8976 (Print) 1362-3028 (Online) Journal homepage: <http://www.tandfonline.com/loi/tmph20>

Measurements and calculations of H₂-broadening and shift parameters of water vapour transitions of the $\nu_1 + \nu_2 + \nu_3$ band

T. M. Petrova, A. M. Solodov, A. A. Solodov, V. M. Deichuli & V. I. Starikov

To cite this article: T. M. Petrova, A. M. Solodov, A. A. Solodov, V. M. Deichuli & V. I. Starikov (2018) Measurements and calculations of H₂-broadening and shift parameters of water vapour transitions of the $\nu_1 + \nu_2 + \nu_3$ band, Molecular Physics, 116:10, 1409-1420, DOI: [10.1080/00268976.2018.1432905](https://doi.org/10.1080/00268976.2018.1432905)

To link to this article: <https://doi.org/10.1080/00268976.2018.1432905>



Published online: 01 Mar 2018.



Submit your article to this journal [↗](#)



Article views: 22

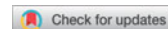


View related articles [↗](#)



View Crossmark data [↗](#)

RESEARCH ARTICLE



Measurements and calculations of H₂-broadening and shift parameters of water vapour transitions of the $\nu_1 + \nu_2 + \nu_3$ band

T. M. Petrova^a, A. M. Solodov^a, A. A. Solodov^a, V. M. Deichuli^{a,b} and V. I. Starikov^{c,d}

^aDepartment of Spectroscopy, V.E. Zuev Institute of Atmospheric Optics, Tomsk, Russia; ^bDepartment of Photonics and Informatics, National Research Tomsk State University, Tomsk, Russia; ^cDepartment of Advanced Mathematics, Tomsk State University of Control System and Radio Electronics, Tomsk, Russia; ^dDepartment of Informational Systems, National Research Tomsk Polytechnic University, Tomsk, Russia

ABSTRACT

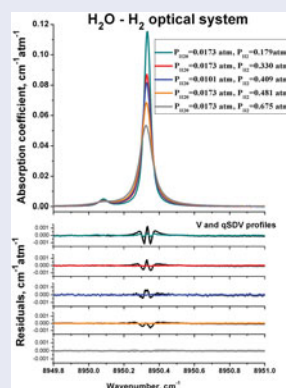
The water vapour line broadening and shifting for 97 lines in the $\nu_1 + \nu_2 + \nu_3$ band induced by hydrogen pressure are measured with Bruker IFS 125 HR FTIR spectrometer. The measurements were performed at room temperature, at the spectral resolution of 0.01 cm⁻¹ and in a wide pressure range of H₂. The calculations of the broadening γ and shift δ coefficients were performed in the semi-classical method framework with use of an effective vibrationally depended interaction potential. Two potential parameters were optimised to improve the quality of calculations. Good agreements with measured broadening coefficients were achieved. The comparison of calculated broadening coefficients γ with the previous measurements is discussed. The analytical expressions that reproduce these coefficients for rotational, ν_2 , ν_1 , and ν_3 vibrational bands are presented.

ARTICLE HISTORY

Received 24 October 2017
Accepted 17 January 2018

KEYWORDS

Fourier transform spectroscopy; line broadening and shift coefficients; semi-classical method; intermolecular potential; water vapour



1. Introduction

Knowledge of the water vapour absorption spectra in the presence of the hydrogen and helium gases is necessary for many applications. Water vapour has been detected in many objects of the Solar System, including Venus, Mars, and comets, and was observed in the IR spectra of brown dwarfs, red giant stars, and cold dark molecular clouds. Hydrogen and helium are present in the atmospheres of the giant planets, and they are the dominant constituents of the Sun.

Nowadays, the experimental hydrogen broadening coefficients of H₂O transitions have been obtained in different spectral regions [1–6]. The primary experimental work on water broadened by hydrogen is by Brown

and Plymate [2], who recorded and analysed spectra of pure rotational and three vibrational bands ν_1 , ν_2 , and ν_3 between 55 and 4045 cm⁻¹. The pure rotational transitions have been examined in [1] and [3], respectively. The vibration–rotational transitions of $2\nu_1$, $\nu_1 + \nu_3$ and $2\nu_1 + \nu_2 + \nu_3$ vibrational bands have been investigated in [5,6] and [4]. The temperature dependence of some broadening coefficients was studied in [1,5,7,8]. The calculations of the broadening coefficients γ for 386 pure rotational transitions were performed in [9]. The calculations were compared with the measurements of pure rotational and ν_2 band [2] and a good agreement (better than 2% and 4% on average) was observed.

Our previous analysis of the coefficients γ obtained for 17 and 15 vibrational bands of H₂O in the

Table 1. Experimental conditions.

Spectrum number	Spectral resolution (cm ⁻¹)	Partial pressure of H ₂ O (atm)	Partial pressure of H ₂ (atm)	Temperature (K)
1	0.01	0.01013(3)	0.409(2)	296.0(5)
2	0.01	0.01735(4)	0.179(1)	295.8(5)
3	0.01	0.01735(4)	0.330(2)	296.0(5)
4	0.01	0.01735(4)	0.481(2)	295.9(5)
5	0.01	0.01735(4)	0.675(3)	295.7(5)

broadening case of water vapour transitions by He and Ar, respectively [10–12], showed the strong dependence of the broadening coefficients γ on the stretching vibrational modes excitation in H₂O molecule. In [10], we found that the temperature dependence of the calculated coefficients γ in the case of the H₂O lines broadening by the light atom He is determined by the used isotropic potential depth.

In this work, we begin the investigation of H₂-broadening of water vapour transitions in a wide spectral region. In the first step, we studied 97 transitions from the 8600 to 9070 cm⁻¹ region which belongs to the $\nu_1 + \nu_2 + \nu_3$ vibrational band.

For these transitions, we measured the broadening, γ , shift, δ , and narrowing, β^0 , coefficients. The coefficients γ and δ were calculated and compared with experimental data for studied transitions and for transitions from other spectral regions investigated in [1–8]. For the rotational, ν_2 , ν_1 , and ν_3 vibrational bands, we proposed the analytical expressions that reproduce the broadening coefficients γ .

2. Experimental and fitting procedure

The water vapour absorption spectra in 8600–9070 cm⁻¹ region perturbed by H₂ pressure were measured using Bruker IFS 125HR high-resolution Fourier transform spectrometer located in V.E. Zuev Institute of Atmospheric Optics SB RAS. The spectrometer was equipped with CaF₂ beam splitter, Si detector and tungsten halogen lamp as the light source. The White-type multiple reflection absorption cell with BaF₂ windows and with gold-coated mirrors was used for the measurements. The records of the H₂O and H₂O–H₂ absorption spectra were made at room temperature with the optical path length of 1280 cm and unapodised resolution 0.01 cm⁻¹, which corresponds to 90 cm of MOPD in the Bruker definition. The signal-to-noise ratio (expressed as the maximum signal amplitude divided by the RMS noise amplitude) was calculated using the standard procedure of the OPUS 6.5 software. The average value of the RMS noise amplitude in the spectral region under study was 0.0032 giving a signal-to-noise ratio of 3100 for an absorbance

of around 1.0. It was obtained by the coaddition of 1200 interferograms. The pressure of the water vapour was 0.0101 and 0.0173 atm and was measured with a Baratron gauge with an estimated uncertainty of 0.25%. The pressure of the H₂O–H₂ mixture ranged between 0.179 and 0.675 atm and was measured with the manometer DVR-5 (1100 mbar full scale) which has a stated uncertainty of 0.5% according to the manufacturer. All measurements are summarised in Table 1.

The numbers between parentheses represent the absolute uncertainty in units of the last digit quoted.

In a number of cases, the Voigt profile does not give a fully accurate representation of the spectral line shape and its use can lead to a systematic underestimation of line intensities [13,14]. The version of HITRAN 2016 database [15] has line parameters for non-Voigt profiles for several molecules including H₂O. Our analysis of several line profiles has shown that for a qualitative description of the water vapour spectra measured in this work, the quadratic speed-dependent Voigt (hereinafter qSDV) profile is sufficient. For the determination of the spectral line parameters, we used a program that allows us deriving the line parameters from their simultaneous fitting to several spectra recorded under different conditions [16]. We derived the broadening, shift and narrowing coefficients using the subroutine where new fast algorithms implementing a quadratic speed dependence of collisional width and shift were developed [17].

The fitting procedure was performed without taking account of the instrumental line shape (ILS). For our measurements, the spectral resolution was chosen in such a way as to minimise the ILS influence on retrieved line parameters. It was 0.01 cm⁻¹. We tested the retrieved line parameters (broadening coefficients and intensities) of several H₂O lines for two cases (with ILS and without) and obtained that the difference does not exceed 0.5%.

In Figure 1, the profiles of two H₂O absorption lines [3 2 1] ← [2 0 2] and [7 2 6] ← [6 2 5] of $\nu_1 + \nu_2 + \nu_3$ vibrational band and respective residual between the experimental and calculated spectra are presented. The lower panels show the residuals between the experimental and calculated spectra for the Voigt and the speed-dependent Voigt profiles. It can be seen from the figure that the use

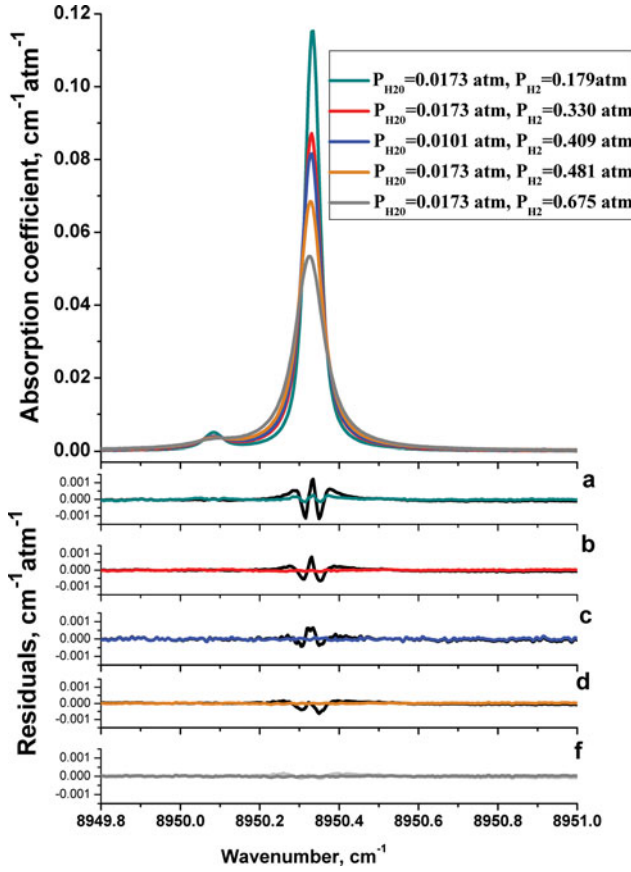


Figure 1. Example of the experimental spectra (upper panel) and the residuals between the experimental and calculated spectra for the Voigt and the speed-dependent Voigt profiles ((a) $P_{\text{H}_2\text{O}} = 0.0173$ atm, $P_{\text{H}_2} = 0.179$ atm; (b) $P_{\text{H}_2\text{O}} = 0.0173$ atm, $P_{\text{H}_2} = 0.330$ atm; (c) $P_{\text{H}_2\text{O}} = 0.0101$ atm, $P_{\text{H}_2} = 0.409$ atm; (d) $P_{\text{H}_2\text{O}} = 0.0173$ atm, $P_{\text{H}_2} = 0.481$ atm; (f) $P_{\text{H}_2\text{O}} = 0.0173$ atm, $P_{\text{H}_2} = 0.675$ atm).

of the speed-dependent Voigt profile has made it possible to simulate simultaneously the five experimental spectra close to or within the noise level. In total, the broadening parameters for 97 lines of $\nu_1 + \nu_2 + \nu_3$ band of the main water isotopologue were obtained. Table 2 shows line parameters of the water molecule: broadening, shift, and narrowing coefficient.

3. Calculation method

The line broadening and the line-centre shift coefficients, γ and δ , respectively, were calculated in the Robert-Bonamy (RB) formalism [18] by using the following expression:

$$\begin{aligned} \gamma_{if} + i\delta_{if} = & \frac{n}{c} \sum_2 \rho_2 \int_0^\infty v F(v) dv \int_{r_0}^\infty Dr_c dr_c \\ & \times [1 - \exp(-iS_1 - S_{2,i}^{\text{outer}} - S_{2,f}^{\text{outer}} \\ & - S_{2,\text{middle}}'')]. \end{aligned} \quad (1)$$

Here, $F(v)$ is the Maxwell-Boltzmann velocity distribution (normalised to unity), n is the buffer gas density, c is the speed of light, ρ_2 is the Boltzmann factor for perturbing molecules in the state J_2 (normalised to $\sum_2 \rho_2 = 1$), v is the relative velocity of the two molecules and r_c is the closest approach distance between them. Formulas for the parameter r_0 , the Jacobian D of the transition from the variable (b, v) (b is the impact parameter) to the variable (r_c, v) are presented in [15]. The real and imaginary parts of resonance functions from $S_2(b)$ were obtained in the exact trajectories model [19,20]. To calculate these functions, as well as $S_1(b)$ and $S_2(b)$, we used an effective inter-action potential

$$\begin{aligned} \tilde{V}^{(n)}(R) = & \tilde{V}_{\mu-q}^{(n)}(R) + V_{q-q}(R) + {}^{\text{mod}}\tilde{V}_{\text{isot}}^{(n)}(R) \\ & + V_{\text{anisot}}^{aa}(R) \end{aligned} \quad (2)$$

which is determined for a given vibrational state (n) = (ν_1, ν_2, ν_3) of H_2O molecule; ν_1, ν_2 , and ν_3 are the vibrational quantum numbers. In Equation (2), the first two contributing terms are the dipole (H_2O)-quadrupole (H_2) and quadrupole (H_2O)-quadrupole (H_2) electrostatic interactions [21] with the vibrationally depended dipole moment $\mu(n)$ [22] of H_2O molecule. The vibrational dependence of the H_2O molecule quadrupole moments components is unknown, and for each vibrational state (n), they were fixed to the values $q_{xx} = -0.13$, $q_{yy} = -2.5$, $q_{zz} = 2.63$ (in 10^{-26} esu) [9]. For M_2 molecule, we used $q = 0.65 \times 10^{-26}$ esu $\cdot \text{\AA}$ [23].

The model isotropic potential

$$\begin{aligned} {}^{\text{mod}}\tilde{V}_{\text{isot}}^{(n)}(R) = & 4\tilde{\varepsilon}^{(n)} \left[-\frac{(\tilde{\sigma}^{(n)})^6}{R^6} + \frac{(\tilde{\sigma}^{(n)})^{12}}{R^{12}} \right] \\ = & -\tilde{C}_6^{(n)}/R^6 + \tilde{C}_{12}^{(n)}/R^{12} \end{aligned} \quad (3)$$

with the quantities $\tilde{C}_6^{(n)} = 4\tilde{\varepsilon}^{(n)} \cdot (\tilde{\sigma}^{(n)})^6$ and $\tilde{C}_{12}^{(n)} = 4\tilde{\varepsilon}^{(n)} \cdot (\tilde{\sigma}^{(n)})^{12}$ depends on the vibrational (n) = (ν_1, ν_2, ν_3) and rotational ($J, K \equiv K_a$) quantum numbers of H_2O molecule [24]. Here, $\tilde{\varepsilon}^{(n)}$ and $\tilde{\sigma}^{(n)}$ are the parameters which are defined in the way that ${}^{\text{mod}}\tilde{V}_{\text{isot}}^{(n)}(R = \tilde{\sigma}^{(n)}) = 0$ and $\tilde{\varepsilon}^{(n)}$ is depth of ${}^{\text{mod}}\tilde{V}_{\text{isot}}^{(n)}(R)$. The isotropic potential (3) is used in the calculations of the resonance functions from $S_2(b)$ in the exact trajectory model and in the calculation of the n -dependend lower limit of integration

$$r_0(n) = \sigma(n) \cdot \left\{ \frac{2}{1 + \sqrt{1 + m v^2 / 2\varepsilon(n)}} \right\}^{1/6} \quad (4)$$

in the second integral of Equation (1). The parameter r_0 vibrational dependence, introduced in Equation (20)

Table 2. Broadening, γ , shift, δ , and narrowing, β^0 , coefficients (in $\text{cm}^{-1} \text{atm}^{-1}$) of the $\nu_1 + \nu_2 + \nu_3$ band of H_2O molecule induced by hydrogen pressure, $T = 296 \text{ K}$.

$\nu \text{ (cm}^{-1}\text{)}$	$(1,1,1)JK_aK_c$	JK_aK_c	$\gamma \text{ (exp)}$	$\gamma \text{ (cal)}$	$\gamma \text{ (sur)}$	$\delta \text{ (exp)}$	$\delta \text{ (cal)}$	β^0
8830.230794	1 0 1	0 0 0	0.0898(3)	0.0970	0.0918	- 0.0107(1)	- 0.01097	0.0044(1)
8783.204617	0 0 0	1 0 1	0.0905(3)	0.0970	0.0918	- 0.0133(2)	- 0.01095	0.0049(1)
8848.069247	2 1 2	1 1 1	0.0914(4)	0.0885	0.0886	- 0.0104(1)	- 0.01193	0.0051(2)
8861.124017	2 1 1	1 1 0	0.0887(4)	0.0914	0.0886	- 0.0085(1)	- 0.01162	0.0062(2)
8760.139985	1 0 1	2 0 2	0.0857(5)	0.0901	0.0860	- 0.0162(1)	- 0.01156	0.0064(2)
8869.872043	3 0 3	2 0 2	0.0801(5)	0.0839	0.0773	- 0.0088(1)	- 0.01226	0.0053(1)
8765.039188	1 1 1	2 1 2	0.0925(6)	0.0885	0.0886	- 0.0134(2)	- 0.01189	0.0064(2)
8823.999372	2 1 1	2 1 2	0.0920(4)	0.0884	0.0873	- 0.0057(1)	- 0.01191	0.0042(2)
8754.931633	1 1 0	2 1 1	0.0891(4)	0.0914	0.0886	- 0.0137(2)	- 0.01158	0.0038(1)
8790.030432	2 1 2	2 1 1	0.0939(3)	0.0884	0.0873	- 0.0156(1)	- 0.01192	0.0033(1)
8879.117690	3 2 2	2 2 1	0.0786(4)	0.0769	0.0799	- 0.0121(2)	- 0.01340	0.0054(2)
8808.468200	2 2 1	2 2 0	0.0785(5)	0.0758	0.0790	- 0.0141(2)	- 0.01343	0.0051(1)
8877.257665	3 2 2	3 0 3	0.0840(3)	0.0807	0.0822	- 0.0051(1)	- 0.01307	0.0029(2)
8742.927875	2 1 2	3 1 3	0.0805(4)	0.0804	0.0848	- 0.0167(2)	- 0.01271	0.0051(1)
8837.394971	3 1 2	3 1 3	0.0855(4)	0.0832	0.0816	- 0.0081(2)	- 0.01246	0.0040(1)
8882.871875	4 1 4	3 1 3	0.0679(4)	0.0719	0.0778	- 0.0102(1)	- 0.01375	0.0040(1)
8730.129948	2 1 1	3 1 2	0.0867(4)	0.0869	0.0848	- 0.0124(1)	- 0.01203	0.0064(2)
8772.295769	3 1 3	3 1 2	0.0879(4)	0.0832	0.0816	- 0.0159(1)	- 0.01245	0.0039(1)
9021.164737	4 3 1	3 1 2	0.0807(4)	0.0811	0.0794	- 0.0110(2)	- 0.01334	0.0038(1)
8733.806629	2 2 0	3 2 1	0.0790(4)	0.0810	0.0799	- 0.0157(1)	- 0.01279	0.0040(1)
8717.910077	3 0 3	4 0 4	0.0728(4)	0.0754	0.0680	- 0.0173(1)	- 0.01313	0.0048(1)
8854.877536	4 1 3	4 1 4	0.0778(5)	0.0767	0.0737	- 0.0109(2)	- 0.01317	0.0045(1)
8713.657050	3 2 2	4 2 3	0.0720(4)	0.0737	0.0783	- 0.0141(2)	- 0.01371	0.0059(2)
8821.155579	4 2 2	4 2 3	0.0736(3)	0.0763	0.0762	- 0.0108(1)	- 0.01336	0.0026(2)
8917.679045	5 2 4	4 2 3	0.0673(5)	0.0684	0.0736	- 0.0143(1)	- 0.01442	0.0083(2)
8933.462535	5 2 3	4 2 2	0.0763(4)	0.0780	0.0736	- 0.0152(1)	- 0.01313	0.0062(2)
8715.879487	3 3 1	4 3 2	0.0635(4)	0.0658	0.0694	- 0.0171(1)	- 0.01470	0.0036(2)
8928.477481	5 3 3	4 3 2	0.0636(4)	0.0663	0.0696	- 0.0145(1)	- 0.01486	0.0059(1)
8714.765900	3 3 0	4 3 1	0.0648(4)	0.0674	0.0694	- 0.0173(1)	- 0.01448	0.0039(1)
8932.529379	5 3 2	4 3 1	0.0656(3)	0.0703	0.0696	- 0.0098(2)	- 0.01427	0.0050(1)
8817.413261	4 4 0	4 4 1	0.0503(3)	0.0495	0.0579	- 0.0154(2)	- 0.01670	0.0047(2)
8936.261664	5 4 2	4 4 1	0.0538(4)	0.0567	0.0595	- 0.0123(2)	- 0.01597	0.0044(2)
8817.369130	4 4 1	4 4 0	0.0497(4)	0.0496	0.0579	- 0.0160(2)	- 0.01669	0.0035(1)
8936.409310	5 4 1	4 4 0	0.0533(3)	0.0571	0.0595	- 0.0119(1)	- 0.01593	0.0032(1)
8698.524898	4 1 4	5 1 5	0.0594(4)	0.0633	0.0696	- 0.0176(2)	- 0.01464	0.0039(1)
8680.258403	4 1 3	5 1 4	0.0743(5)	0.0772	0.0696	- 0.0135(2)	- 0.01302	0.0051(2)
9065.648011	6 3 3	5 1 4	0.0744(4)	0.0723	0.0695	- 0.0094(1)	- 0.01434	0.0039(2)
8689.222317	4 2 3	5 2 4	0.0607(5)	0.0686	0.0736	- 0.0192(4)	- 0.01427	0.0039(4)
8833.033335	5 2 3	5 2 4	0.0702(3)	0.0726	0.0705	- 0.0126(1)	- 0.01373	0.0028(1)
8675.007199	4 2 2	5 2 3	0.0740(2)	0.0781	0.0736	- 0.0114(1)	- 0.01301	0.0022(1)
8771.530665	5 2 4	5 2 3	0.0726(4)	0.0724	0.0705	- 0.0139(1)	- 0.01376	0.0039(2)
8953.479398	6 2 4	5 2 3	0.0742(4)	0.0743	0.0674	- 0.0090(1)	- 0.01352	0.0043(1)
8685.718499	4 3 1	5 3 2	0.0659(4)	0.0701	0.0696	- 0.0152(2)	- 0.01417	0.0044(1)
8956.293475	6 3 3	5 3 2	0.0679(5)	0.0699	0.0670	- 0.0145(2)	- 0.01423	0.0055(2)
8957.195568	6 4 3	5 4 2	0.0561(5)	0.0595	0.0609	- 0.0141(2)	- 0.01576	0.0067(2)
8695.179815	4 4 0	5 4 1	0.0547(4)	0.0568	0.0595	- 0.0171(1)	- 0.01582	0.0035(2)
8957.866830	6 4 2	5 4 1	0.0557(4)	0.0605	0.0609	- 0.0143(1)	- 0.01561	0.0036(1)
8675.048062	5 0 5	6 0 6	0.0557(5)	0.0564	0.0525	- 0.0164(2)	- 0.01533	0.0082(2)
8675.778921	5 1 5	6 1 6	0.0521(5)	0.0554	0.0618	- 0.0177(1)	- 0.01551	0.0048(2)
8925.221614	7 1 7	6 1 6	0.0495(4)	0.0477	0.0551	- 0.0147(2)	- 0.01658	0.0072(2)
8658.078344	5 1 4	6 1 5	0.0673(4)	0.0696	0.0618	- 0.0148(2)	- 0.01389	0.0042(1)
8955.053804	7 1 6	6 1 5	0.0597(5)	0.0613	0.0551	- 0.0131(2)	- 0.01507	0.0048(1)
8665.129942	5 2 4	6 2 5	0.0582(5)	0.0624	0.0674	- 0.0148(2)	- 0.01496	0.0049(1)
8685.418992	6 0 6	6 2 5	0.0581(5)	0.0567	0.0613	- 0.0162(2)	- 0.01526	0.0052(1)
8950.332968	7 2 6	6 2 5	0.0545(4)	0.0566	0.0610	- 0.0150(2)	- 0.01578	0.0057(2)
8646.468583	5 2 3	6 2 4	0.0739(3)	0.0744	0.0674	- 0.0111(2)	- 0.01335	0.0031(1)
8662.015715	5 3 3	6 3 4	0.0609(5)	0.0632	0.0670	- 0.0144(1)	- 0.01505	0.0057(1)
8966.967639	7 3 5	6 3 4	0.0586(6)	0.0593	0.0629	- 0.0145(1)	- 0.01561	0.0056(1)
8654.823001	5 3 2	6 3 3	0.0680(4)	0.0698	0.0670	- 0.0140(1)	- 0.01410	0.0038(1)
8982.758659	7 3 4	6 3 3	0.0707(5)	0.0683	0.0629	- 0.0168(1)	- 0.01431	0.0069(2)
8667.644633	5 4 2	6 4 3	0.0553(4)	0.0594	0.0609	- 0.0151(1)	- 0.01558	0.0038(2)
8977.364389	7 4 4	6 4 3	0.0560(4)	0.0577	0.0600	- 0.0141(1)	- 0.01596	0.0035(1)
8666.763334	5 4 1	6 4 2	0.0564(3)	0.0602	0.0609	- 0.0151(1)	- 0.01547	0.0027(2)
8979.528470	7 4 3	6 4 2	0.0587(2)	0.0600	0.0600	- 0.0135(2)	- 0.01565	0.0020(1)
8652.086844	6 0 6	7 0 7	0.0473(4)	0.0482	0.0469	- 0.0170(2)	- 0.01627	0.0044(1)
8937.232964	8 0 8	7 0 7	0.0434(5)	0.0421	0.0429	- 0.0150(2)	- 0.01716	0.0047(2)
8652.401802	6 1 6	7 1 7	0.0469(3)	0.0479	0.0551	- 0.0168(2)	- 0.01634	0.0031(1)
8937.130021	8 1 8	7 1 7	0.0429(4)	0.0420	0.0498	- 0.0154(2)	- 0.01720	0.0037(1)
8636.757067	6 1 5	7 1 6	0.0607(4)	0.0613	0.0551	- 0.0156(1)	- 0.01486	0.0062(2)

(Continued)

Table 2. (Continued).

ν (cm ⁻¹)	(1,1) JK_aK_c	JK_aK_c	γ (exp)	γ (cal)	γ (sur)	δ (exp)	δ (cal)	β^0
8967.231607	8 17	7 16	0.0526(4)	0.0543	0.0498	-0.0146(1)	-0.01587	0.0039(1)
8964.612451	8 27	7 26	0.0493(1)	0.0517	0.0554	-0.0150(1)	-0.01629	0.0010(1)
8996.796807	8 2 6	7 2 5	0.0672(4)	0.0644	0.0554	-0.0135(1)	-0.01462	0.0044(2)
8636.037304	6 3 4	7 3 5	0.0571(2)	0.0594	0.0629	-0.0138(2)	-0.01539	0.0023(1)
8983.704959	8 3 6	7 3 5	0.0562(4)	0.0552	0.0582	-0.0148(2)	-0.01604	0.0037(1)
9004.172134	8 3 5	7 3 4	0.0720(5)	0.0659	0.0582	-0.0145(2)	-0.01450	0.0060(2)
8996.438807	8 4 5	7 4 4	0.0559(1)	0.0549	0.0576	-0.0131(2)	-0.01625	0.0009(1)
8636.970977	6 4 2	7 4 3	0.0601(4)	0.0597	0.0600	-0.0152(1)	-0.01548	0.0041(1)
9001.653937	8 4 4	7 4 3	0.0648(5)	0.0597	0.0576	-0.0123(1)	-0.01556	0.0066(1)
8646.769909	6 5 1	7 5 2	0.0541(2)	0.0537	0.0534	-0.0148(1)	-0.01627	0.0022(1)
9004.405906	8 5 3	7 5 2	0.0562(2)	0.0536	0.0537	-0.0133(1)	-0.01649	0.0015(1)
8948.149069	9 0 9	8 0 8	0.0403(3)	0.0380	0.0401	-0.0150(1)	-0.01756	0.0033(1)
8948.441322	9 1 9	8 1 8	0.0411(4)	0.0379	0.0459	-0.0151(1)	-0.01760	0.0043(2)
8978.737816	9 1 8	8 1 7	0.0475(2)	0.0485	0.0459	-0.0143(2)	-0.01650	0.0023(1)
8978.857194	9 2 8	8 2 7	0.0486(4)	0.0474	0.0507	-0.0143(2)	-0.01673	0.0041(1)
9010.063240	9 2 7	8 2 6	0.0620(4)	0.0581	0.0507	-0.0120(1)	-0.01534	0.0044(1)
8609.830584	7 3 5	8 3 6	0.0567(5)	0.0553	0.0582	-0.0137(2)	-0.01578	0.0049(2)
8998.964254	9 3 7	8 3 6	0.0544(5)	0.0517	0.0538	-0.0150(2)	-0.01635	0.0043(1)
8611.380803	7 4 4	8 4 5	0.0588(4)	0.0550	0.0576	-0.0154(1)	-0.01599	0.0062(1)
9014.129783	9 4 6	8 4 5	0.0580(3)	0.0521	0.0545	-0.0138(2)	-0.01650	0.0050(2)
9023.206397	9 5 5	8 5 4	0.0583(4)	0.0512	0.0527	-0.0142(2)	-0.01673	0.0038(1)
8603.308511	8 0 8	9 0 9	0.0420(3)	0.0382	0.0401	-0.0165(2)	-0.01722	0.0049(2)
8958.634012	10 0 10	9 0 9	0.0461(3)	0.0350	0.0385	-0.0135(2)	-0.01784	0.0033(1)
8603.399440	8 1 8	9 1 9	0.0419(5)	0.0382	0.0459	-0.0161(1)	-0.01726	0.0052(1)
8957.600523	10 1 10	9 1 9	0.0436(1)	0.0350	0.0432	-0.0160(2)	-0.01788	0.0109(2)
8989.799122	10 1 9	9 1 8	0.0460(4)	0.0448	0.0432	-0.0148(1)	-0.01682	0.0042(1)
9022.866783	10 2 8	9 2 7	0.0582(5)	0.0524	0.0472	-0.0101(2)	-0.01602	0.0045(1)
8998.715111	11 2 10	10 2 9	0.0460(3)	0.0412	0.0448	-0.0152(1)	-0.01729	0.0059(1)

^a γ (cal) and δ (cal) were calculated with Potential 4 from Table 3; γ (sur) denotes that coefficients γ were calculated according to Equations (19)–(21). The set of the parameters for γ (sur) is listed in Table 8; values of ν and quantum assignments are from HITRAN 2016 [15]; between parentheses, the estimated uncertainty is in the last quoted digit units.

of [18], substantially influences the calculated vibrational dependence of the broadening coefficients γ and δ .

The last term in Equation (2)

$$V_{anisot}^{aa}(R) = \sum_{q=0}^4 \sum_{l_1=1}^2 \sum_{m_1=-l_1}^{l_1} \sum_{l_2=0}^{l_1} \sum_{m=-\inf\{l_1, l_2\}}^{m=\inf\{l_1, l_2\}} \left\{ \frac{|m_1|}{|m|} b_q^{l_1 l_2} \frac{|m_1| D_{12+q}^{l_1 l_2}}{R^{12+q}} - \frac{|m_1|}{|m|} c_q^{l_1 l_2} \frac{|m_1| E_{6+q}^{l_1 l_2}}{R^{6+q}} \right\} D_{mm_1}^{l_1}(\Omega_1) D_{-m_0}^{l_2}(\Omega_2) \quad (5)$$

is an anisotropic part of an atom–atom potential [25]. This part does not depend on n . The constants $\binom{\dots}{\dots} b_{\dots}^{\dots}$, $\binom{\dots}{\dots} c_{\dots}^{\dots}$ as well as the quantities $\binom{\dots}{\dots} D_{\dots}^{\dots}$, $\binom{\dots}{\dots} E_{\dots}^{\dots}$ which depend on the atom–atom force parameters e_{H-H} , e_{O-H} , d_{H-H} and d_{O-H} are defined in [25]. The expressions for $S_2(b)$ functions that correspond to the potential (5) are given in [20,25].

The interruption function $S_1(b)$ in Equation (1) is determined by the difference $\text{mod } \tilde{V}_{isot}^{(n)}(R) - \text{mod } \tilde{V}_{isot}^{(0)}(R)$ of the effective isotropic potential (3) in the excited (n) and ground vibrational ($n=0$) = (0, 0, 0) states, respectively, and it is written as

$$S_1 = \frac{3\pi}{8v\hbar r_c^5} \left[-a_6 \Delta C_6 + a_{12} \frac{21}{32} \frac{\Delta C_{12}}{r_c^6} \right], \quad (6)$$

where $\Delta C_p = \tilde{C}_p^{(n)} - \tilde{C}_p^{(n=0)}$ and the constants a_p ($p=6, 12$) are defined in [10]. In Equation (3), each $\tilde{C}_p^{(n)} = \tilde{C}_p^{(1)}(n) + C_p^{(2)}$, where the upper subscripts (1) and (2) determine the contribution from the induction + dispersion and isotropic atom–atom potential, respectively. The contribution $C_p^{(2)}$ does not depend on n and thus the vibrotational dependence of an effective isotropic potential (3) is determined by the vibrotational dependence of the effective induction + dispersion potential.

The long-range part of this potential may be expressed by the effective molecular quantities as

$$\begin{aligned} \binom{(n)}{\dots} \tilde{V}_{isot, long}^{ind-disp}(R) &= -\frac{\tilde{C}_6^{(1)}(n)}{R^6} \\ &= -\frac{[\tilde{\mu}(n)^2 + 3/2u \cdot \tilde{\alpha}(n)] \cdot \alpha_2}{R^6}. \end{aligned} \quad (7)$$

Here, $\tilde{\mu}(n)$ and $\tilde{\alpha}(n)$ are the effective dipole moment and mean polarisability of H₂O molecule, $u = u_1 u_2 / (u_1 + u_2)$, $\alpha_2 = 0.767 \text{ \AA}^3$ [23] is the polarisability of H₂ and u_1 and u_2 are the ionisation energies of H₂O and H₂, respectively.

The effective dipole moment $\tilde{\mu}(n)$ was taken as

$$\begin{aligned} \tilde{\mu}(n) &= \mu(v_1, v_2, v_2) + h_{200}(0, v_2, 0) \cdot J(J+1) \\ &\quad + h_{020}(0, v_2, 0) \cdot K_a^2. \end{aligned} \quad (8)$$

Table 3. The sets of the atom–atom and isotropic potential parameters for H₂O–H₂ system obtained for the H₂O molecule rotational band^a.

	Pot.1	Pot.2	Pot.3	Pot.4	Pot.5	Pot.6
ε/k_B (K)	10.0	50.0	80.0	110.0	130.0	150.0
σ (Å)	3.15	2.91	2.86	2.84	2.83	2.82
$e_{\text{H-H}}$	4.4	4.0	4.0	4.0	4.2	4.0
$e_{\text{O-H}}$	7.0	7.0	7.0	7.0	7.0	7.0
$d_{\text{H-H}}$	860.	860.	860.	860.	860.	860.
$d_{\text{O-H}}$	3700.	3700.	3700.	3700.	3700.	3700.
rms_γ	3.3×10^{-3}	3.3×10^{-3}	3.3×10^{-3}	3.1×10^{-3}	3.1×10^{-3}	3.2×10^{-3}
D_{12}	1.20	1.09	1.04	0.99	0.96	0.93
β	5.9×10^{-3}	6.5×10^{-3}	6.9×10^{-3}	7.2×10^{-3}	7.5×10^{-3}	7.7×10^{-3}

^a Parameters $e_{\text{H-H}}$, $e_{\text{O-H}}$ and $d_{\text{H-H}}$, $d_{\text{O-H}}$ are given in 10^{-12} erg·Å⁶ and 10^{-12} erg·Å¹², respectively; rms_γ is given in cm^{-1} atm⁻¹; diffusion coefficient D_{12} and dynamic friction coefficient β are defined in cm^2/s and cm^{-1} atm⁻¹, respectively.

The values of $\mu(v_1, v_2, v_3)$ are presented in [22]. The terms with the constants $h_{200}(0, v_2, 0)$ and $h_{020}(0, v_2, 0)$ from [26] determine the dipole moment rotational dependence, J and K_a are rotational quantum numbers of H₂O molecule. The effective mean polarisability $\tilde{\alpha}(n)$ was taken in the form

$$\tilde{\alpha}(n) = \alpha(v_1, v_2, v_3) + \Delta\alpha^{(J)} \cdot J(J+1) + \Delta\alpha^{(K)} K_a^2. \quad (9)$$

The values of the parameters $\Delta\alpha^{(J)}$ and $\Delta\alpha^{(K)}$ presented in [20,27]. In [28], the vibrational dependence of mean polarisability $\alpha(v_1, v_2, v_3)$ was determined as

$$\alpha(v_1, v_2, v_3) = 1.4613 + 0.042 \cdot v_1 + 0.013 \cdot v_2 + 0.042 \cdot v_3 (\text{Å}^3). \quad (10)$$

In our approach, $\Delta C_6 = \Delta C_6^{(1)}(n) - \Delta C_6^{(1)}(n=0)$ and thus

$$\Delta C_6 = [\tilde{\mu}^2(f) - \tilde{\mu}^2(i) + 3/2u(\tilde{\alpha}(f) - \tilde{\alpha}(i))\alpha_2], \quad (11)$$

where $\tilde{\mu}(f)$, $\tilde{\mu}(i)$ and $\tilde{\alpha}(f)$, $\tilde{\alpha}(i)$ are the dipole moments and mean polarisabilities of H₂O molecule in the final (f) = $(v_1, v_2, v_3)[J_f K_{af} K_{cf}]$ and initial (i) = $(0, 0, 0)[J_i K_{ai} K_{ci}]$ vibrational–rotational states in the transition (i) → (f), respectively. According to Equations (8), (9) and (11), the quantity ΔC_6 may be presented as $\Delta C_6 = \Delta C_6^{vib} + \Delta C_6^{rot}$ with

$$\Delta C_6^{vib} = C_6(n) - C_6(0) = [\mu^2(v_1, v_2, v_3) - \mu^2(0, 0, 0) + 3/2u(\alpha(v_1, v_2, v_3) - \alpha(0, 0, 0))]\alpha_2, \quad (12)$$

$$\Delta C_6^{rot} \approx C_6^{(J)} \cdot [J_f(J_f+1) - J_i(J_i+1)] + C_6^{(K)} \cdot [K_{af}^2 - K_{ai}^2]. \quad (13)$$

In the last equation,

$$C_6^{(J)} = [2 \cdot \mu(v_1, v_2, v_3) \cdot h_{200} + 3/2u \cdot \Delta\alpha^{(J)}]\alpha_2,$$

$$C_6^{(K)} = [2 \cdot \mu(v_1, v_2, v_3) \cdot h_{020} + 3/2u \cdot \Delta\alpha^{(K)}]\alpha_2. \quad (14)$$

The relation of the quantity $\Delta C_{12} = \tilde{C}_{12}^{(n)} - \tilde{C}_{12}^{(n=0)} = \Delta C_{12}^{vib} + \Delta C_{12}^{rot}$ with molecular parameters of H₂O molecule is unknown. In our calculations, the rotational contribution ΔC_{12}^{rot} in ΔC_{12} was fixed to zero value.

4. The choice of potential parameters

In our approach, the used effective interaction potential (2) depends on the vibrational state (n) of H₂O molecule. The choice of potential parameters was stated for the potential with $n = 0$, that is for the ground vibrational state of H₂O. In this case, the effective isotropic potential (3) difference in the excited (n) and ground vibrational state is equal to zero value, so in Equation (6), $\Delta C_6^{vib} = \Delta C_{12}^{vib} = 0$. Potential parameters for electrostatic interactions are described in Section 3. Potential parameters $e_{\text{O-H}}$, $d_{\text{H-H}}$ and $d_{\text{O-H}}$ from the anisotropic atom–atom potential (5) were fixed to the values calculated according to combination rules [29] from the known parameters ε_{ii} and σ_{ii} [30], $i = \text{O or H}$. Three parameters, $e_{\text{H-H}}$ from the potential (5) and ε and σ from the isotropic potential (3) were considered as variable parameters. The parameter ε/k_B was fixed to different values from the interval $10.0 \leq \varepsilon/k_B \leq 150K$, then σ and $e_{\text{H-H}}$ were selected by hands in the way that give the minimum of the quantity.

$$rms_\gamma = \left\{ \sum_{i=1}^N \frac{(\gamma_i^{(\text{exp})} - \gamma_i^{(\text{cal})})^2}{N} \right\}^{1/2} \quad (15)$$

for $N = 63$ broadening coefficient γ , measured [2] and calculated for the pure rotational band. Some of the potential parameters sets are given in Table 2.

Presented in Table 3, rms_γ corresponds to the quantity $\chi_\gamma = 100\% \cdot \sum_{i=1}^N [(\gamma_i^{(\text{exp})} - \gamma_i^{(\text{cal})})/\gamma_i^{(\text{exp})}]/N \cong 0.5\%$,

Table 4. Calculated and experimental [29] diffusion coefficients D_{12} (cm^2/s) for $\text{H}_2\text{O}-\text{H}_2$ system.

T ($^\circ\text{C}$)	Pot.1	Pot.2	Pot.3	Pot.4	Pot.5	Pot.6	Exp.
34.4	1.27	1.16	1.11	1.05	1.02	0.99	0.91
55.5	1.45	1.30	1.24	1.18	1.16	1.12	0.99
79.2	1.60	1.46	1.38	1.33	1.30	1.25	1.10

i.e. the agreement with experimental data is good. Table 3 shows that parameters of an atom–atom and isotropic potentials are determined unambiguously from the experimental half-widths. As the various sets of potential parameters give approximately the same results, two additional criteria formulated in [10] for $\text{H}_2\text{O}-\text{He}$ system were tested in the present work for $\text{H}_2\text{O}-\text{H}_2$ system.

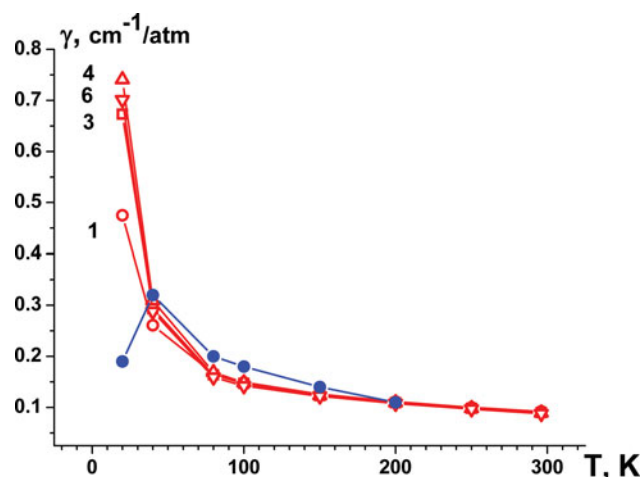
The first criterion has to do with the coefficients which determine the gases transport properties [29]. Parameters ε and σ from the isotropic potential (3) are used in the literature for the calculation of the second virial coefficient, the diffusion coefficients D_{12} , etc. [29]. The last two lines of Table 4 present the calculated diffusion and dynamic friction coefficient β , defined as

$$\beta = \frac{k_B T}{2\pi cm D_{12}}, \quad (16)$$

where m is the H_2O molecule mass, T is the temperature. This parameter is usually compared with the narrowing parameter β^0 , which appears in the profiles where the narrowing effect is taken into account (see, for example, [20]). Because of β^0 data lack, the comparison is made with experimental coefficients D_{12} (Table 3).

According to Table 3, Potential 6 gives the coefficients D_{12} which are the most close to their experimental values.

The second criterion has to do with the temperature dependence of calculated broadening coefficients. The fact is that different potentials give the different calculated temperature dependence of calculated coefficients γ . To study the function $\gamma(T)$ dependence on the used potential

**Figure 2.** Temperature dependence of half-width for rotational [1 0 1] \rightarrow [1 1 0] transition of H_2O line broadening by H_2 . The dark and empty symbols denote the experimental [7] and calculated data. The numbers identify the potential used (see Table 3).

parameters, 11 rotational transitions were chosen. Calculations were made for the temperature 200, 250, 296, 400, and 750 K. The expression

$$\gamma(T) = \gamma(T_0) \cdot (T_0/T)^n \quad (17)$$

with reference temperature $T_0 = 296$ K was used to find the temperature exponent, n . In Table 5, the temperature exponents, n , determined in this study are presented and comparison with other data is given. According to this table, the deviations between n calculated in the present study and in [9], respectively, are not significant for the potentials with $\varepsilon/k_B \geq 80$ K (Potentials 3–6).

Performed calculations of $\gamma(T)$ demonstrated that this function strongly depends on the chosen potential for the low temperature $T < 200$ K. As an example, the comparison with experimental data [1,7] for the transitions [1 0 1] \rightarrow [1 1 0] (556 GHz), [2 2 0] \rightarrow [3 1 3] (183 GHz), respectively, is presented in Figures 2 and 3. To plot experimental data in Figure 2, the expression

Table 5. Temperature exponents for H_2O broadened by H_2

$J'K'_a'K'_c'$	$J''K''_a''K''_c''$	Pot.2	Pot.3	Pot.4	Pot.5	Pot.6	Ref. [9]	Exp. [1, 5]
101	0 0 0	0.56	0.58	0.6	0.61	0.61	0.718(38)	0.87(4)
211	2 1 2	0.52	0.54	0.55	0.57	0.58	0.644(36)	1.02(27)
220	3 1 3	0.47	0.51	0.54	0.53	0.55	0.590(52)	0.95(7)
414	3 2 1	0.45	0.49	0.52	0.51	0.52	0.543(51)	0.85(5)
312	3 2 1	0.51	0.53	0.57	0.56	0.57	0.609(13)	0.40(10)
321	3 2 2	0.47	0.49	0.51	0.52	0.54	0.533(56)	0.62(16)
330	3 3 1	0.35	0.39	0.40	0.44	0.45	0.361(53)	0.35(13)
413	4 2 2	0.49	0.52	0.51	0.55	0.56	0.584(27)	1.5(5)
432	4 3 1	0.38	0.43	0.44	0.46	0.47	0.414(84)	0.39(11)
514	5 2 3	0.46	0.49	0.53	0.48	0.54	0.545(30)	0.72(20)
533	5 3 2	0.38	0.42	0.44	0.46	0.49	0.407(75)	0.25(10)

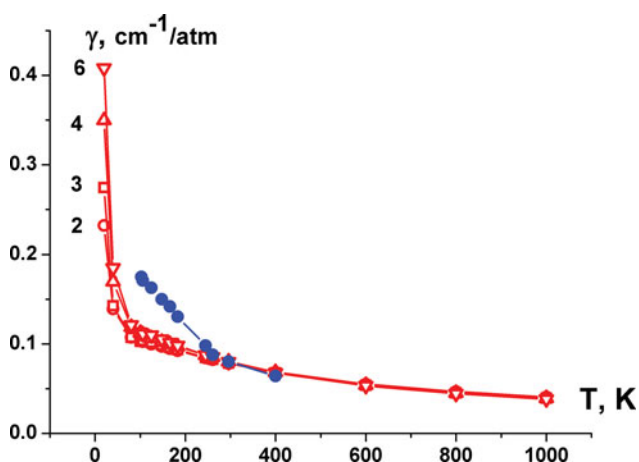


Figure 3. The same as on Figure 2 but for the rotational line $[2\ 2\ 0] \rightarrow [3\ 1\ 3]$.

$\gamma(T) = 4.543(\text{MHz/Torr}) (200/T)^{0.8042}$ obtained in [7] was used. As in the case of $\text{H}_2\text{O}-\text{He}$ system [10], the different potentials for $\text{H}_2\text{O}-\text{H}_2$ system give the different temperature dependence of the coefficients γ for low temperatures.

For all potentials, the agreement between calculated and measured in [1,7], coefficients γ is not good for T approximately smaller than 200 K. For the temperatures $T > 300$ K, the used potential influence on the calculated temperature dependence of γ is not significant. Thus, two additional discussed criteria do not help to choose unique isotropic potential. Potential 4 was taken in our calculations as base potential because its parameters ε and σ are close to those calculated according to combination rules. According to these rules, $\varepsilon/k_B = 109$ K, $\sigma = 2.844$ Å for $\varepsilon_{\text{H}_2\text{O}}/k_B = 356$ K, $\sigma_{\text{H}_2\text{O}} = 2.725$ Å, $\varepsilon_{\text{H}_2}/k_B = 33.3$ K, $\sigma_{\text{H}_2} = 2.968$ Å [29].

In the effective interaction potential (2), these parameters depend on the vibrational state (n) while the parameters, $e_{\text{H}-\text{H}}$, $e_{\text{O}-\text{H}}$, $d_{\text{H}-\text{H}}$, and $d_{\text{O}-\text{H}}$ do not depend on (n).

The calculations of the broadening coefficients γ and δ for 97 lines of the $\nu_1 + \nu_2 + \nu_3$ band were stated with the base Potential 4 of Table 3 and with the quantity ΔC_6 calculated according to Equations (10)–(14). We found out that calculated coefficients $\gamma(\text{cal})$ underestimate experimental coefficient $\gamma(\text{exp})$. The calculations quality improvement may be obtained by the variation of the isotropic potential (3) parameter ε or σ . We fixed $\varepsilon/k_B = 110$ K and then we selected by hands $\sigma = 2.827$ Å to obtain the minimum of rms_γ (15). Similarly, we found out that calculated line shift coefficients δ are greater than experimental ones. This means that the quantity $\Delta C_{12}^{\text{vib}}$ which determines the vibrational dependence of the isotropic potential (3) short-range part has to be taken into account in Equation (6). We selected by hands the value $\Delta C_{12}^{\text{vib}} = 500.0\text{D}^2 \cdot \text{Å}^9$ to obtain the minimum of rms_δ which is defined by formula (15) where the symbol δ has to be used instead of symbol γ . Obtained in this way, optimal parameters σ and $\Delta C_{12}^{\text{vib}}$ as well as rms_γ and rms_δ are presented in the seventh line of Table 6. Calculated coefficients γ and δ are listed in the corresponding columns of Table 2.

5. Comparison with other measurements

Because of the experimental data lack in the literature for the studied band, the direct comparison of present data with other data is impossible. However, the comparison may be made for transitions having the same sets of rotational quantum numbers for the lower and final vibrational states. For $N = 86$, such transitions from [2] for the ratio $R_\gamma = \gamma(\text{Present})/\gamma$ [2] (where γ [2] are the broadening coefficients from [2] measured at $T = 291$ K for the ν_1 band), the following statistical data are found:

$$0.95 < R_\gamma < 1.05 \text{ for } N = 71 \text{ transitions.}$$

The mean value of $\chi_\gamma = |R_\gamma - 1| \cdot 100\%$ is 3.3%, and for $N = 71$ transitions, $\chi_\gamma < 5\%$.

Table 6. Optimal parameters σ (Å) and $\Delta C_{12}^{\text{vib}}$ ($\text{D}^2 \cdot \text{Å}^9$) minimising rms_γ and rms_δ for eight vibrational bands $(0,0,0) \rightarrow (\nu_1, \nu_2, \nu_3)$ of H_2O lines perturbed by H_2 . Other potential parameters are defined by the Potential 4 from Table 3.

(ν_1, ν_2, ν_3)	σ	$\Delta C_{12}^{\text{vib}}$	rms_γ	rms_δ	N	
(0,0,0)	2.79	0.0	7.4×10^{-3}	–	39	[1]
(0,0,0)	2.84	0.0	3.1×10^{-3}	–	63	[2]
(0,1,0)	2.84	0.0	3.2×10^{-3}	–	274	[2]
(1,0,0)	2.82	250.0	4.3×10^{-3}	–	103	[2]
(0,0,1)	2.82	250.0	3.9×10^{-3}	–	182	[2]
(1,1,1)	2.827	500.0	3.7×10^{-3}	2.5×10^{-3}	97	Present
(1,0,1)	2.812	500.0	5.7×10^{-3}	–	8	[5]
(1,0,1)	2.83	500.0	4.7×10^{-3}	3.9×10^{-3}	4	[6]
(2,0,0)	2.72	500.0	19.8×10^{-3}	–	4	[5,6]
(2,1,1)	2.820	600.0	7.3×10^{-3}	4.7×10^{-3}	14	[4]

N is the number of lines under study.

Table 7. Comparison of measured and calculated broadening γ and shift δ coefficients for different vibrational bands $(0,0,0) \rightarrow (v_1, v_2, v_3)$ of H_2O molecule perturbed by hydrogen pressure.

(v_1, v_2, v_3) $(1,0,1)JK_aK_c$	$(0,0,0)JK_aK_c$	$\gamma(\text{exp.})^a$	$\gamma(\text{cal.})$	$\gamma(\text{Present})/\gamma$ [6]	$\delta(\text{exp.})^a$	$\delta(\text{cal.})$
212	313	0.0728	0.0799	1.10	-0.0155	-0.010
303	322	0.0741	0.0795		-0.0146	-0.010
515	514	0.0682	0.0686		-0.0122	-0.011
660	661	0.0430	0.0372		-0.0100	-0.014
$(1,0,1)JK_aK_c$	$(0,0,0)JK_aK_c$	$\gamma(\text{exp.})^b$	$\gamma(\text{cal.})$	$\gamma(\text{Present})/\gamma$ [5]	$\delta(\text{exp.})$	$\delta(\text{cal.})$
000	101	0.0930	0.0994	0.97		-0.009
212	211	0.1010	0.0905	0.93		-0.009
322	321	0.0880	0.0809			-0.010
330	331	0.0630	0.0632			-0.012
331	330	0.0650	0.0633			-0.012
431	432	0.0640	0.0703			-0.011
432	431	0.0700	0.0702			-0.011
532	533	0.0670	0.0702			-0.011
$(2,0,0)JK_aK_c$	$(0,0,0)JK_aK_c$					
101	110	0.0832 ^a	0.1070		-0.014 ^a	-0.008
321	312	0.0860 ^b	0.1003			-0.008
422	413	0.1230 ^b	0.0972			-0.009
523	514	0.1040 ^b	0.0927			-0.009
$(2,1,1)JK_aK_c$	$(0,0,0)JK_aK_c$	$\gamma(\text{exp.})^c$	$\gamma(\text{cal.})$	$\gamma(\text{Present})/\gamma$ [4]	$\delta(\text{exp.})$	$\delta(\text{cal.})$
110	111	0.0925	0.0933		-0.010	-0.015
101	202	0.0849	0.0923	1.01	-0.020	-0.015
110	211	0.0874	0.0934	1.02	-0.015	-0.015
202	303	0.0836	0.0864		-0.015	-0.016
313	312	0.1010	0.0853		-0.015	-0.016
321	322	0.0785	0.0812		-0.017	-0.017
303	404	0.0861	0.0777	0.85	-0.020	-0.017
322	423	0.0785	0.0763	0.92	-0.017	-0.018
422	423	0.0747	0.0787	0.99	-0.007	-0.018
331	432	0.0671	0.0685	0.95	-0.015	-0.019
404	505	0.0735	0.0679		-0.022	-0.019
414	515	0.0671	0.0658	0.89	-0.025	-0.019
533	532	0.0532	0.0698		-0.027	-0.019
515	616	0.0595	0.0580	0.88	-0.022	-0.021

^a [6].^b [5].^c [4].

The comparison with $N = 8$ coefficients γ measured in [4] for the $2\nu_1 + \nu_2 + \nu_3$ band, with $N = 2$ coefficients of $\nu_1 + \nu_3$ band from [5] and with one coefficient of this band from [6] is presented in the fifth column of Table 7. The simultaneous comparison of present experimental data with those obtained for the other vibrational bands [2,4,5,6] is given in Figure 4.

In the next step, the comparison was made between calculated coefficients γ and δ and experimental data for these coefficients obtained for rotational band [3], ν_1, ν_2 , and ν_3 , $\nu_1 + \nu_3$, $2\nu_1$ [5,6] and $2\nu_1 + \nu_2 + \nu_3$ [4] bands. For the last three bands, only separate coefficients γ are measured. For each vibrational band $(0,0,0) \rightarrow (v_1, v_2, v_3)$, parameters ε/k_B , $e_{\text{H-H}}$, $e_{\text{O-H}}$, $d_{\text{H-H}}$, and $d_{\text{O-H}}$ were fixed to the values presented in the fifth column of Table 2 (Potential 4), and only one parameter $\sigma(v_1, v_2, v_3)$ was selected to find the minimum of rms_γ (15). The quantity $\Delta C_6^{vib}(v_1, v_2, v_3)$ was fixed to the value calculated according to Equation (12). If the data on the shift coefficients δ

are absent for a given band, then the quantity ΔC_{12}^{vib} was fixed to the value calculated according to the formula

$$\Delta C_{12}(v_1, v_2, v_3) = 250.0 \cdot v_1 + 0.0 \cdot v_2 + 250.0 \cdot v_3 (D^2 \text{Å}^9). \quad (18)$$

This formula is based on the value $\Delta C_{12}^{vib}(1,1,1) = 500.0D^2 \text{Å}^9$ obtained for the $(0,0,0) \rightarrow (1,1,1)$ band. We suppose that the excitation of the stretching modes in H_2O molecules (ν_1 and ν_3 quantum numbers) influences the shifts coefficients in the same way but the excitation of the bending mode (ν_2 quantum number) is negligible. For the $(0,0,0) \rightarrow (2,1,1)$ band, the quantity ΔC_{12}^{vib} was selected by hands to find the minimum rms_δ . Obtained potential parameters are presented in Table 6.

The comparison with measured coefficients is given in Table 7.

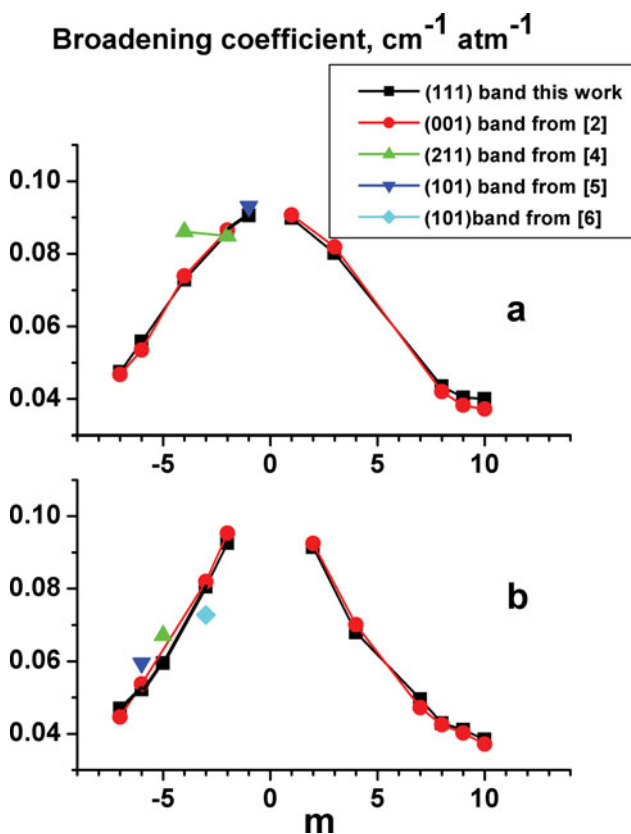


Figure 4. Experimental values of H₂O broadening coefficients as a function of rotational quantum number m , $m = J'' + 1$ for R branch and $m = -J''$ for P-branch (J'' is the rotational quantum number of lower vibrational state); (a) for sub-branch $(J 0 J) \leftrightarrow (J-1 0 J-1)$; (b) for sub-branch $(J 1 J) \leftrightarrow (J-1 1 J-1)$.

Some details are revealed in this comparison.

- (1) Calculated broadening coefficients γ are in good agreement with $N = 622$ coefficients $\gamma(\text{exp})$ measured by Brown and Plymate [2] for four vibrational bands. For the $\nu_1 + \nu_3$ band, the good agreement is for $N = 8$ and for $N = 4$ coefficients $\gamma(\text{exp})$ obtained in [5,6], respectively.
- (2) Calculated broadening coefficients γ are not simultaneously in a good agreement with $\gamma(\text{exp})$ measured in [2] and [3], respectively, for the same rotational band. This shows the quantity rms_γ from the second and third lines of Table 6. The calculated coefficients γ underestimate $\gamma(\text{exp})$ systematically from [3] (Figure 5). The maximal deviation between $\gamma(\text{cal})$ and $\gamma(\text{exp})$ was achieved for the line with $N = 19$ ($\nu = 446.3508 \text{ cm}^{-1}$) with $\gamma(\text{cal})/\gamma(\text{exp}) = 0.59$.
- (3) There are big discrepancies between $\gamma(\text{cal})$ and $\gamma(\text{exp})$ measured for $2\nu_1$ [5,6] and $2\nu_1 + \nu_2 + \nu_3$ [4] bands. In particular, for the line $[3 1 3] \leftarrow [3 1 2]$ ($\nu = 12,113.883 \text{ cm}^{-1}$) and $[5 3 3] \leftarrow [5 3 2]$ ($\nu = 12,136.517 \text{ cm}^{-1}$) of the $2\nu_1 + \nu_2 + \nu_3$ band,

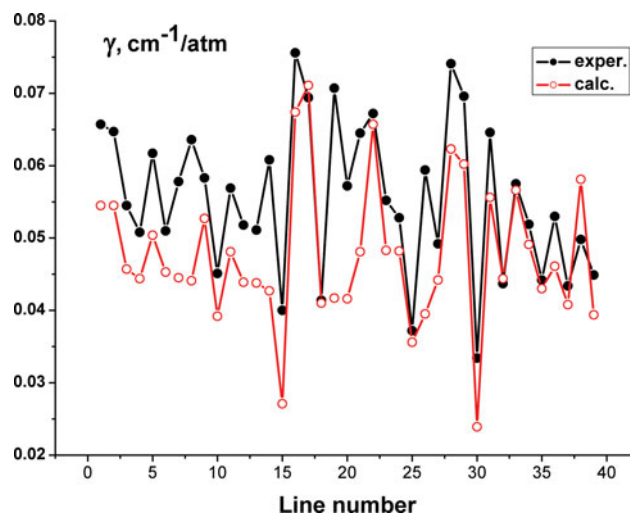


Figure 5. Calculated and experimental [3] broadening coefficients γ for the rotational lines of H₂O molecule broadened by H₂. The lines are ordered according to Table 2 of [3].

the ratio $\gamma(\text{cal})/\gamma(\text{exp}) = 0.837$ and 1.294 , respectively. For other 12 lines, $0.89 < \gamma(\text{cal})/\gamma(\text{exp}) < 1.08$.

A very small ratio $\gamma(\text{cal})/\gamma(\text{exp}) = 0.62$ and 0.69 , with $\gamma(\text{exp})$ from [5] was obtained for the lines $[4 1 3] \leftarrow [4 2 2]$ and $[5 1 4] \leftarrow [5 2 3]$ from the $2\nu_1$ band. The coefficients $\gamma(\text{exp})$ consistence measured in [2] and [5] for the lines with the same sets of rotational quantum numbers but for the different vibrational bands are discussed also in [2]. In particular, for these two lines, $\gamma(\text{exp [5]})/\gamma(\text{exp [2]}) = 1.62$ and 1.45 , respectively, [2].

6. Analytical representation of the broadening coefficients γ

The hydrogen broadening and shift coefficients γ and δ were calculated for the transitions of the rotational, ν_1 , ν_2 , ν_3 and $\nu_1 + \nu_1 + \nu_3$ vibrational bands with the rotational quantum numbers J'' and K_a'' up to 10 for $T = 296 \text{ K}$. To represent the broadening coefficients γ , we used the analytical formula [20]

$$\gamma(\text{sur}) = x_2 \{ 1/\cosh[x_3(K' - x_4)] + 1/\cosh[x_3(K'' - x_4)] \}, \quad (19)$$

where the quantities x_k depend on the rotational J' , $K' \equiv K_a'$, J'' , $K'' \equiv K_a''$ quantum numbers via the relations

$$x_2 = (x_{20} + x_{21} \cdot |K' - K''|) / \text{Cosh}[x_{22} \cdot (J' + J'')] + x_{23} \cdot (J' + J'')^2, \quad (20)$$

Table 8. Parameters of model $\gamma(sur)$ obtained in the fitting of the model (19)–(21) to the calculated + experimental H₂-broadening coefficients of H₂O vibrational bands (0,0,0) \rightarrow (ν_1, ν_2, ν_3), $T = 296$ K^a.

	(0,0,0) or (0,1,0)	(1,0,0)	(0,0,1)	(1,1,1)
x_{20}	$0.4273(37) \times 10^{-1}$	$0.4732(56) \times 10^{-1}$	$0.4770(38) \times 10^{-1}$	$0.4630(35) \times 10^{-1}$
x_{21}	$0.3433(258) \times 10^{-2}$	$0.3322(173) \times 10^{-2}$	$0.1548(107) \times 10^{-2}$	$0.1839(114) \times 10^{-2}$
x_{22}	$0.9673(186) \times 10^{-1}$	$0.1076(33)$	$0.9380(242) \times 10^{-1}$	$0.9227(230) \times 10^{-1}$
x_{23}	$-0.1832(90) \times 10^{-2}$	$-0.2190(149) \times 10^{-2}$	$-0.1613(118) \times 10^{-2}$	$-0.1551(113) \times 10^{-2}$
x_{30}	$0.5004(132)$	$0.7243(392)$	$0.4935(169)$	$0.4696(166)$
x_{31}	$-0.1363(78) \times 10^{-1}$	$-0.4999(560) \times 10^{-1}$	$-0.1604(111) \times 10^{-1}$	$-0.1475(98) \times 10^{-1}$
x_{32}	0.0	$0.1192(191) \times 10^{-2}$	0.0	0.0
x_{41}	$0.2212(16)$	$0.2245(43)$	$0.2221(28)$	$0.2222(20)$

^a Parameters x_{20} and x_{21} are expressed in $\text{cm}^{-1} \text{atm}^{-1}$, while the other parameters are dimensionless, $x_{40} = x_{42} = 0$.

$$x_k = [x_{k0} + x_{k1} \cdot (J' + J'') + x_{k2} \cdot (J' + J'')^2], k = 3, 4. \quad (21)$$

The set of the parameters x_{kl} , $k = 2, 3, 4$ and $l = 0, 1, 2, 3$ of the model (19)–(21) was determined by the least squares method from the fitting of expressions (19)–(21) to the calculated ($J'', K_a'' \leq 10$) and experimental ([2] and the present study) values of the broadening coefficients γ for each band separately. The obtained parameters sets are listed in Table 8 and the coefficients γ calculated according to the model (19)–(21) for the $\nu_1 + \nu_2 + \nu_3$ band are given in the sixth column of Table 1.

7. Discussions

The experimental data on the broadening coefficients γ and δ for the 97 most intensive lines of the $\nu_1 + \nu_2 + \nu_3$ vibrational band of H₂O molecule were obtained in the analysis of the H₂O–H₂ absorption spectra, recorded from 8600 to 9070 cm^{-1} with the help of IFS 125HR Fourier spectrometer at room temperature, spectral resolution of 0.01 cm^{-1} and in the wide pressure range of H₂.

In the calculations of γ and δ , the vibrationally depended intermolecular potential (2), (3), (5) of H₂O–H₂ system was taken.

We revealed that the vibrational dependence of the calculated broadening coefficients is due mainly to the effective isotropic potential (3) vibrational dependence. In the present work, we used vibrationally depended parameter $\sigma(n)$ from this potential. The minimums of rms_γ (15) for different vibrational bands were found for different $\sigma(n)$ (Table 6). This parameter as well as $\varepsilon(n)$ determines the low integration limit $r_0(n)$ (4) in the second integral in Equation (1) which is different for different n . Table 6 shows the $\sigma(n)$ decreasing trend with the number of the stretching vibration quanta ν_1 and ν_3 . This decreasing leads to the r_0 (4) decreasing and to the increasing of the calculated broadening coefficients γ and $|\delta|$.

The vibrational dependence of the dipole moment $\mu(n)$ (8) and the mean polarisability $\alpha(n)$ (10) of H₂O molecule determine the vibrational dependence of the quantity ΔC_6^{vib} (12) from the interruption function $S_1(b)$ (6) which strongly affects the calculated shift coefficients δ . For each vibrational band, the quantity ΔC_6^{vib} was calculated according to known values for $\mu(n)$ and $\alpha(n)$ (10). We found that the quantity ΔC_{12}^{vib} from $S_1(b)$ (6) which determines the vibrational dependence of the isotropic potential (3) short-range part has to be taken into account to achieve agreements between calculated and experimental shift coefficients δ . We also found that the function $S_1(b)$ (6) does not influence significantly the calculated broadening coefficients γ .

The potential parameters from Table 6 predict well the data for the broadening coefficients γ obtained for four vibrational bands in [2] and for the $\nu_1 + \nu_2 + \nu_3$ vibrational band investigated in the present work. However, according to Table 6, the prediction of the coefficients γ for pure rotational transitions investigated in [3] is not accurate. There are big discrepancies between $\gamma(cal)$ and $\gamma(exp)$ measured for some transitions in the $2\nu_1$, [5,6] and $2\nu_1 + \nu_2 + \nu_3$ [4] bands. The reason for this is not clear.

The model $\gamma(sur)$ (19)–(21) with the parameters from Table 8 may be used in the calculations of the broadening coefficients γ for the transitions $[J_i K_{ai} K_{ci}] \rightarrow [J_f K_{af} K_{cf}]$ with different sets of the rotational quantum numbers J_i , $K_{ai} \leq 10$ for four vibrational bands, noted in Table 8, $T = 296$ K.

Disclosure statement

No potential conflict of interest was reported by the authors.

Funding

Russian Foundation for Basic Research [grant number 15-02-06808].

References

- [1] J.M. Dutta, C.R. Jones, T.M. Goyette, and F.C. De Lucia, *Icarus* **102**, 232 (1993). doi:10.1006/icar.1993.1046.
- [2] L.R. Brown and C. Plymate, *J. Quant. Spectrosc. Radiat. Transfer* **56**, 263 (1996). doi:10.1016/0022-4073(95)00191-3.
- [3] D.W. Steyert, W.F. Wang, J.M. Sirota, N.M. Donahue, and D.C. Reuter, *J. Quant. Spectrosc. Radiat. Transfer* **83**, 183 (2004). doi:10.1016/S0022-4073(02)00300-X.
- [4] A. Lucchesini, S. Gozzini, and C. Gabbanini, *Eur. Phys. J. D* **8**, 223 (2000). doi:10.1007/s10053-000-8807-z.
- [5] S. Langlois, T.P. Birbeck, and R.K. Hanson, *J. Mol. Spectrosc.* **167**, 272 (1994). doi:10.1006/jmsp.1994.1234.
- [6] V. Zeninari, B. Parvite, D. Courtois, N.N. Lavrentieva, Y.N. Ponomarev, and G. Durry, *Mol. Phys.* **102**, 1697 (2004). doi:10.1080/00268970412331287133.
- [7] M.J. Dick, B.J. Drouin, and J.C. Pearson, *J. Quant. Spectrosc. Radiat. Transfer* **110**, 619 (2009). doi:10.1016/j.jqsrt.2008.11.012.
- [8] A. Faure, L. Wiesenfeld, B.J. Drouin, and J. Tennyson, *J. Quant. Spectrosc. Radiat. Transfer* **116**, 79 (2013). doi:10.1016/j.jqsrt.2012.09.015.
- [9] R.R. Gamache, R. Lynch, and L.R. Brown, *J. Quant. Spectrosc. Radiat. Transfer* **56**, 471 (1996). doi:10.1016/0022-4073(96)00098-2.
- [10] T.M. Petrova, A.M. Solodov, A.A. Solodov, and V.I. Starikov, *J. Quant. Spectrosc. Radiat. Transfer* **129**, 241 (2013). doi:10.1016/j.jqsrt.2013.06.021.
- [11] T.M. Petrova, A.M. Solodov, A.A. Solodov, V.M. Deichuli, and V.I. Starikov, *J. Mol. Spectrosc.* **331**, 60 (2017). doi:10.1016/j.jms.2016.11.006.
- [12] T.M. Petrova, A.M. Solodov, A.A. Solodov, V.M. Deichuli, and V.I. Starikov, *Mol. Phys.* **115**, 1642 (2017). doi:10.1080/00268976.2017.1311422.
- [13] J.-M. Hartmann, C. Boulet, and D. Rober, *Collisional Effects on Molecular Spectra: Laboratory Experiments and Models, Consequences for Application* (Elsevier Science, Amsterdam, 2008).
- [14] D. Lisak, A. Cygan, D. Bermejo, J.L. Domenech, J.T. Hodges, and H. Tran, *J. Quant. Spectrosc. Radiat. Transfer* **164**, 221 (2015). doi:10.1016/j.jqsrt.2015.06.012.
- [15] I.E. Gordon, L.S. Rothman, C. Hil, R.V. Kochanov, Y. Tan, P.F. Bernath, M. Birk, V. Boudon, A. Campargue, K.V. Chance, B.J. Drouin, J.-M. Flaud, R.R. Gamache, J.T. Hodges, D. Jacquemart, V.I. Perevalov, A. Perrin, K.P. Shine, M.-A.H. Smith, J. Tennyson, G.C. Toon, H. Tran, V.G. Tyuterev, A. Barbe, A.G. Császár, V.M. Devi, T. Furtenbacher, J.J. Harrison, J.-M. Hartmann, A. Jolly, T.J. Johnson, T. Karman, I. Kleiner, A.A. Kyuberis, J. Loos, O.M. Lyulin, S.T. Massie, S.N. Mikhailenko, N. Moazzen-Ahmadi, H.S.P. Mülle, O.V. Naumenko, A.V. Nikitin, O.L. Polyansky, M. Rey, M. Rotger, S.W. Sharpe, K. Sung, E. Starikova, S.A. Tashkun, J. Vander Auwera, G. Wagner, J. Wilzewski, P. Wcisło, S. Yu, E.J. Zak, E.J. Zak b Yu, E.J. Zak b. *J. Quant. Spectrosc. Rad. Transfer* **203**, 3 (2017). doi:10.1016/j.jqsrt.2017.06.038.
- [16] T.M. Petrova, A.M. Solodov, A.P. Shcherbakov, V.M. Deichuli, A.A. Solodov, Yu.N. Ponomarev, and T.Y. Chesnokova, *Atmos. Ocean. Opt.* **30**, 123 (2017). doi:10.1134/S1024856017020105.
- [17] C.D. Boone, *J. Quant. Spectrosc. Radiat. Transfer* **105**, 525 (2007). doi:10.1016/j.jqsrt.2006.11.015.
- [18] D. Robert and J. Bonamy, *J. Phys. (Paris)* **40**, 923 (1979). doi:10.1051/jphys:019790040010092300.
- [19] A.D. Bykov, N.N. Lavrentieva, and L.N. Sinitsa, *Atmos. Ocean. Opt.* **5**, 907 (1992).
- [20] J. Buldyreva, N.N. Lavrentieva, and V.I. Starikov, *Collisional Line Broadening and Shifting of Atmospheric Gases. A Practical Guide for Line Shape Modeling by Current Semi-Classical Approaches* (Imperial College Press, London, 2010).
- [21] R.P. Leavitt, *J. Chem. Phys.* **73**, 5432 (1980). doi:10.1063/1.440088.
- [22] M. Mengel and P. Jensen, *J. Mol. Spectrosc.* **169**, 73 (1995). doi:10.1006/jmsp.1995.1007.
- [23] A.A. Radzik and B.M. Smirnov, *Atomic and Molecular Physics* (Atomizdat, Moscow, 1980 (in Russian)).
- [24] V.I. Starikov, *J. Quant. Spectrosc. Radiat. Transfer* **155**, 49 (2015). doi:10.1016/j.jqsrt.2014.12.018.
- [25] B. Labani, J. Bonamy, D. Robert, J.-M. Hartmann, and J. Taine, *J. Chem. Phys.* **84**, 4256 (1986). doi:10.1063/1.450047.
- [26] V.I. Starikov, *J. Mol. Spectrosc.* **206**, 166 (2001). doi:10.1006/jmsp.2001.8306.
- [27] V.I. Starikov and A.E. Protasevich, *J. Mol. Struct.* **646**, 81 (2003). doi:10.1016/S0022-2860(02)00613-0.
- [28] V.I. Starikov, T.M. Petrova, A.M. Solodov, A.A. Solodov, and V.M. Deichuli, *Eur. Phys. J. D* **71**, 108 (2017). doi:10.1140/epjd/e2017-70685-9.
- [29] J.O. Hirschfelder, C.F. Curtiss, and R.B. Bird, *Molecular Theory of Gases and Liquids* (Wiley, New York, 1967).
- [30] J.P. Bouanich, *J. Quant. Spectrosc. Radiat. Transfer* **47**, 243 (1992). doi:10.1016/0022-4073(92)90142-Q.